Cloning and functional expression of a gene encoding a vacuolar-type proton-translocating pyrophosphatase from *Trypanosoma cruzi*

Janet E. HILL[1], David A. SCOTT, Shuhong LUO and Roberto DOCAMPO[2]

Laboratory of Molecular Parasitology, Department of Pathobiology, College of Veterinary Medicine, University of Illinois at Urbana-Champaign, 2001 South Lincoln Avenue, Urbana, IL 61802, U.S.A.

Acidocalcisomes are acidic Ca^{2+}-storage organelles found in trypanosomatids that are similar to organelles known historically as volutin granules. Acidification of these organelles is driven in part by a vacuolar H^+-pyrophosphatase (V-H^+-PPase), an enzyme that is also present in plant vacuoles and in some bacteria. Here, we report the cloning and sequencing of a gene encoding the acidocalcisomal V-H^+-PPase of *Trypanosoma cruzi*. The protein (*T. cruzi* pyrophosphatase, TcPPase) predicted from the nucleotide sequence of the gene has 816 amino acids and a molecular mass of 85 kDa. Several sequence motifs found in plant V-H^+-PPases were present in TcPPase, explaining its sensitivity to *N*-ethylmaleimide and *N*,*N*′-dicyclohexylcarbodi-imide. Heterologous expression of the cDNA encoding TcPPase in the yeast *Saccharomyces cerevisiae* produced a functional enzyme. Phylogenetic analysis of the available V-H^+-PPase sequences indicates that TcPPase is nearer to the vascular plant cluster and the branch containing *Chara*, a precursor to land plants, than to any of the other pyrophosphatase sequences included in the analysis. The apparent lack of such a V-H^+-PPase in mammalian cells may provide a target for the development of new drugs.

Key words: acidocalcisome, vacuolar pyrophosphatase, volutin granule.

INTRODUCTION

Chagas' disease, the result of infection with the protozoan parasite *Trypanosoma cruzi*, is the leading cause of heart disease in Latin America [1]. Over 18 million people are infected and over 90 million are at risk. Acute Chagas' disease results in myocarditis in approx. 60 % of patients with an estimated 9 % mortality occurring in endemic areas. Most chagasic patients die from heart failure associated with cardiomyopathy during the chronic phase of the disease [1,2] and therapy is unsatisfactory [2]. There is therefore considerable interest in developing novel chemotherapeutic approaches against Chagas' disease based on unique aspects of *T. cruzi* structure and metabolism.

In previous work, we demonstrated the presence of a vacuolar proton-translocating pyrophosphatase (vacuolar H^+-pyrophosphatase or V-H^+-PPase) in acidocalcisomes of *T. cruzi* [3]. Acidocalcisomes are acidic Ca^{2+}-storage organelles found in trypanosomatids and apicomplexan parasites; they are abundant in the intracellular stages of these parasites, and characterized by their high electron density and a high content of polyphosphates, calcium, magnesium, sodium and zinc [4]. These organelles are similar to the volutin granules described almost a century ago in various micro-organisms [4]. Until recently, V-H^+-PPases had been described in detail only in plants, algae, archea and thermophilic bacteria, along with a homologous H^+-pyrophosphate synthase in the photosynthetic bacterium *Rhodospirillum rubrum* [5–7]. An apparently vacuolar-type pyrophosphatase activity was detected in rat liver Golgi fractions [8], but the assays were done using very high concentrations of PP_i (1–3 mM) and there is no evidence that the enzyme is similar to the plant, algal or bacterial enzymes. In addition, we have found that V-H^+-PPases with similar characteristics to the plant enzyme are present in other medically important parasites, such as *T. brucei* [9], *Leishmania donovani* [10], *Plasmodium falciparum* [11] and *Toxoplasma gondii* [12], the aetiological agents of African trypanosomiasis, Kala-Azar, malaria and toxoplasmosis, respectively.

Whereas V-H^+-PPase activity has been measured in these parasites, a thorough molecular characterization of this enzyme will be essential for structure–function analysis and further development of potential chemotherapeutic agents. In the present study, we report the cloning, sequencing and heterologous expression in yeast of a *T. cruzi* gene, designated *T. cruzi* pyrophosphatase (*TcPPase*), that encodes a functional V-H^+-PPase. The TcPPase protein sequence indicates that it is an authentic member of the family of V-H^+-PPases as defined in plants and bacteria and provides relevant information concerning the importance of different residues to the susceptibility of the enzyme to different inhibitors.

MATERIALS AND METHODS

Parasites

T. cruzi amastigotes and trypomastigotes (Y strain) were obtained from the culture medium of L_6E_9 myoblasts as we have described before [3]. *T. cruzi* epimastigotes (Y strain) were grown at 28 °C in liver-infusion tryptose (LIT) medium [13] supplemented with 10 % newborn calf serum.

Chemicals

Newborn calf serum, Dulbecco's PBS, acid-washed glass beads (400–600 μm), EGTA, proteinase K, RNase A, leupeptin, *trans*-

Abbreviations used: V-H^+-PPase, vacuolar H^+-pyrophosphatase; TcPPase, *T. cruzi* pyrophosphatase; TcP0, *T. cruzi* ribosomal protein 1; Tos-Lys-CH_2Cl, *N*-α-*p*-tosyl-L-lysine chloromethyl ketone; DCCD, *N*,*N*′-dicyclohexylcarbodi-imide; NEM, *N*-ethylmaleimide; AEBSF, 4-(2-aminoethyl)-benzenesulphonyl fluoride; AMDP, aminomethylenediphosphonate; ORF, open reading frame.

[1] Present address: National Research Council Plant Biotechnology Institute, 110 Gymnasium Place, Saskatoon, Saskatchewan, S7N 0W9, Canada.
[2] To whom correspondence should be addressed (e-mail rodoc@uiuc.edu).

epoxysuccinyl-L-leucylamido-(4-guanidino)butane (E-64), *N*-α-*p*-tosyl-L-lysine chloromethyl ketone (Tos-Lys-CH_2Cl, or 'TLCK'), *N*,*N*′-dicyclohexylcarbodi-imide (DCCD), *N*-ethylmaleimide (NEM) and Hepes were purchased from Sigma (St. Louis, MO, U.S.A.). 4-(2-Aminoethyl)benzenesulphonyl fluoride (AEBSF) was from Calbiochem (San Diego, CA, U.S.A.). Pepstatin came from Boehringer Mannheim (Indianapolis, IN, U.S.A.). Zymolase P20 was from ICN Biomedicals (Irvine, CA, U.S.A.). Yeast media were bought from Bio 101 (Vista, CA, U.S.A.). Trizol reagent, SuperScript PCR buffer and SuperScript II reverse transcriptase were from Gibco Life Technologies (Gaithersburg, MD, U.S.A.). The bacteriophage vector λGEM11, Poly(A) tract mRNA isolation system, proof-reading polymerase, host strain LE392 and the Packagene System were bought from Promega (Madison, WI, U.S.A.). [α-^{32}P]dCTP and [α-^{32}P]UTP (both 3000 Ci/mmol) were from Amersham (Arlington Heights, IL, U.S.A.). pCR2.1-TOPO cloning kit and the yeast strain InvSc1 were from Invitrogen (Carlsbad, CA, U.S.A.). Zeta-Probe GT nylon membranes and the protein assay were from Bio-Rad (Hercules, CA, U.S.A.). The 25f15 cDNA clone was provided generously by Dr Lena Aslund, Department of Medical Genetics, Uppsala University, Uppsala, Sweden (*T. cruzi* Genome Initiative). Aminomethylenediphosphonate (AMDP) [14] was provided kindly by Professor Philip Rea, University of Pennsylvania, Philadelphia, PA, U.S.A. All other reagents were analytical grade.

Genomic DNA isolation

Epimastigotes (100 ml) were harvested by centrifugation and cell pellets were washed once in ice-cold Dulbecco's PBS. The cell pellet was resuspended in 7 ml of TEN (0.1 M NaCl/10 mM Tris/HCl, pH 8.0/1 mM EDTA) with 100 μg/ml proteinase K/0.5 % SDS (w/v), and gently vortexed before incubating at 55 °C for 3 h. The lysate was then treated with RNase A (10 μg/ml) for 30 min at 37 °C. Lysates were extracted once with TE (TEN without NaCl)-saturated phenol, followed by three phenol/chloroform (1:1) extractions and a final chloroform extraction. Genomic DNA was precipitated by the addition of 0.7 ml of 3 M sodium acetate, pH 5.2, and 15 ml of ethanol. After pelleting, the DNA was washed with 70 % ethanol and resuspended in TE buffer before quantification by spectrophotometry.

Southern-blot analysis

Total genomic DNA from *T. cruzi* epimastigotes (10 μg per lane) was digested with *Bam*HI, *Eco*RI, *Sac*I, *Xba*I and *Xho*I, separated on a 0.8 % agarose gel and transferred to a nylon membrane. The blot was probed with a [α-^{32}P]dCTP-labelled 25f15 insert. After hybridization, the blot was washed three times in 1 × SSC/0.1 % SDS (pre-warmed to 65 °C; where 1 × SSC is 0.15 M NaCl/0.015 M sodium citrate).

Genomic DNA library construction and screening

A complete *T. cruzi* genomic library was constructed in bacteriophage vector λGEM11. Total genomic DNA was partially digested with *Sau*3A1, and fragments of greater than 15 kb were purified by agarose gel electrophoresis. Purified insert DNA was ligated into λGEM11 arms pre-digested with *Bam*HI. The ligation reaction was packaged using the Packagene System, and the titre of the package mixture was determined by plating on *Escherichia coli* host strain LE392. For library screening, 3.2×10^5 p.f.u. (approx. three times the contents of the library) were plated at a density of 2×10^4 p.f.u./90-mm plate on host strain LE392. Plaques were allowed to develop to approx. 1.5 mm in diameter before being lifted on to nylon membranes. Membranes were probed with [α-^{32}P]dCTP-labelled probes according to standard procedures. Positive plaques identified in the screen were serially plaqued to homogeneity. In total, 30 positive plaques were identified in the genomic library screen. Several of these were picked and serially re-plaqued for purification. Sequence data from these positive clones, generated using primers designed from the 25f15 sequence, indicated that they contained identical sequence and represented overlapping clones. Some of the clones contained only the C-terminal portion of the TcPPase open reading frame (ORF), downstream of the internal *Bam*HI site (the result of *Sau*3A1 being used to generate library inserts).

Reverse transcriptase PCR

Total RNA was isolated from *T. cruzi* epimastigotes using Trizol reagent according to the manufacturer's instructions. First-strand cDNA synthesis was primed with an oligonucleotide that annealed to a site within the 3′ portion of the *TcPPase* ORF (5′-GGC AAC GCA ACT CTC GTA GT-3′) in a reaction containing 1 mM dNTPs, 2.5 mM $MgCl_2$, 10 mM dithiothreitol, 1 × SuperScript PCR buffer and 200 units of SuperScript II reverse transcriptase. Target sequences were amplified in a standard PCR using the first-strand cDNA as template and primer Tc-5′-SL (5′-GCG GTC CAT AGA ACA GTT TCT GTA C-3′), which annealed to the 5′-spliced leader sequence of *T. cruzi* mRNA, and a downstream primer (5′-GAG AAG CAG TAC GGC AAC AT-3′) that annealed to sequences just upstream of the primer used for first-strand cDNA synthesis. The 2.1-kb product of the amplification reaction was ligated into vector pCR2.1-TOPO for sequence analysis.

Sequence analysis

DNA sequence data were generated at the High Throughput Sequencing and Genotyping Unit of the Keck Center for Comparative and Functional Genomics at the University of Illinois at Urbana-Champaign. Sequence analysis and tree generation were done using the Biology Workbench 3.0 utility (http://biology.ncsa.uiuc.edu), the Wisconsin Package (version 10.0-UNIX, Genetics Computer Group, Madison, WI, U.S.A.) and the programs seqboot, protdist, neighbor and consense within the PHYLIP phylogeny package (version 3.57c, written by J. Felsenstein, 1995). Trees were viewed and converted to graphic format with TreeView (written by R. D. M. Page, 1998). The PSORT program was from Kenta Nakai, University of Tokyo, Tokyo, Japan.

Northern-blot analysis

For the Northern-blot analysis, total RNA was isolated from trypomastigotes, epimastigotes and amastigotes of *T. cruzi* using Trizol reagent according to the manufacturer's instructions. Polyadenylated RNA was obtained with the Poly(A) tract mRNA isolation system. RNA was electrophoresed in 1 % agarose gels with 2.2 M formaldehyde, 40 mM sodium acetate, 5 mM EDTA and 100 mM Mops buffer, pH 8.0. Northern-blot hybridization was done by standard procedures [15]. The *TcP0* (*T. cruzi* ribosomal protein 1) fragment used as a control in Northern blots (see Figure 4, below) was obtained by amplifying *T. cruzi* genomic DNA by PCR, with primers corresponding to nucleotides 3–54 and 918–936 of the sequence of the *TcP0* gene [16]. Densitometric analyses of Northern blots were done with an ISI-

1000 digital imaging system (Alpha Inotech Corp.). Comparison of levels of *TcPPase* transcripts between the different stages was done by taking as a reference the densitometric values obtained with the *TcP0* transcripts and assuming a similar level of expression of this gene in all stages [16]. Similar results were obtained when the densitometric values were compared by taking into account the amount of RNA added to each lane in three different experiments.

Expression in *Saccharomyces cerevisiae*

The complete *TcPPase* ORF was amplified from a genomic clone by PCR using proof-reading polymerase. The primers used in the PCR were designed to generate a 5′ *Hin*dIII site (5′-CGA AGC TTA TGG GTG ACA TGA GAG G-3′) and a 3′ His tag consisting of six His residues (5′-GTC AGT GGT GGT GGT GGT GCT CAA TGT ACC GCA TGA T-3′). The PCR products were initially ligated into pCR2.1-TOPO for sequencing to confirm the presence of the 3′ His tag and to verify correct amplification of the ORF sequence. The PCR product was then ligated into yeast expression vector pYES2, creating pYES2-816-H_6. To create an N-terminal truncation lacking the putative signal sequence, residues 70–816 of the *TcPPase* ORF were amplified using the upstream primer 5′-GCA AGC TTA TGA GTG CCG ACG TTA CA-3′ and the downstream primer described above. The PCR product was ligated into pYES2 creating pYES2-747-H_6. The pYES2-816-H_6 and pYES2-747-H_6 plasmids were used to transform *S. cerevisiae* InvSc1 by standard methods [17], selecting on complete synthetic medium lacking uracil (CSM-Ura).

Yeast preparations

Yeast cultures were grown in CSM-Ura containing 2 % dextrose and then transferred (at $D_{600} = 0.4$) to CSM-Ura containing 1 % raffinose and 2 % galactose to induce *TcPPase* expression. Yeast cells were harvested by centrifugation and washed once in water, and 1 g of cells (wet weight) was resuspended in 0.5 ml of lysis buffer (125 mM sucrose, 50 mM KCl, 4 mM $MgCl_2$, 0.5 mM EDTA, 20 mM K-Hepes, 5 mM dithiothreitol, 0.1 mM AEBSF, 10 μM pepstatin, 10 μM leupeptin, 10 μM E-64 and 10 μM Tos-Lys-CH_2Cl, pH 7.2), in a 50-ml centrifuge tube. Acid-washed glass beads were added to the level of the meniscus, and the yeast cells were lysed by vortexing for 8 min. The beads were washed manually with 3 ml of lysis buffer, and the combined washings centrifuged for 10 min at 10000 ***g***. This pellet, resuspended in lysis buffer, was used in the H^+-PPase assay.

H^+-PPase assays

The proton-pumping activity of expressed H^+-PPase was assayed using Acridine Orange as described in [3], except that the standard buffer used was 120 mM KCl, 2 mM $MgCl_2$, 50 mM K-Hepes and 50 μM EGTA, pH 7.2. For DCCD and NEM susceptibility assays, *T. cruzi* epimastigotes (2 mg) were resuspended in this buffer without $MgCl_2$. Digitonin (20 μM) was added, followed by DCCD or NEM, and Acridine Orange (3 μM). The mixture was stirred in the spectrophotometer for 5 min at 30 °C before addition of $MgCl_2$, just prior to the start of the experiment.

RESULTS

Identification of *T. cruzi* cDNA 25f15

The V-H^+-PPase sequence from *Arabidopsis thaliana* was used in a tBLASTn search of GenBank dbEST. The results of this search indicated that the predicted amino acid sequence encoded by *T. cruzi* expressed sequence tag (EST) clone 25f15 (accession no. AI066208, 217 nt) was 77 % similar to the corresponding region of the *Arabidopsis* V-H^+-PPase sequence. Determination of the complete sequence of the 25f15 insert indicated that its total size was approx. 800 bp. The ORF portion of the insert corresponds to the C-terminal 190 residues of TcPPase.

Genomic Southern blot of *T. cruzi*

The 25f15 cDNA clone was used as a probe in a genomic Southern blot of total genomic DNA from *T. cruzi* epimastigotes. A single hybridizing band was identified in each lane (results not shown), suggesting that *TcPPase* is present in a single copy in the genome (see below).

Construction and screening of a complete genomic library of *T. cruzi*

Based on an estimated genome size of 80–90 Mb and an average insert size of 20 kb, at least 1.8×10^4 clones were required in the library for complete coverage of the genome. Titration of the library indicated that it contained 1.2×10^5 independent clones. The number of positive plaques identified in the screen (30) is consistent with the *TcPPase* gene being present in a single copy in the genome, because three times the total number of independent clones in the library were plated and the library contains approx. 10 times the genome contents, for a total of a 30-fold representation of the genome. Genomic clone λ11-4 was found to contain the entire ORF. A Southern blot of digested λ11-4 DNA was performed to identify a subfragment of this genomic clone containing the entire *TcPPase* ORF. A 3.7-kb *Pst*I fragment was identified for subcloning. This *Pst*I fragment was ligated into pBluescriptKS(−) (resulting in clone pBS11-4.4P, Figure 1A) and its complete sequence was determined (GenBank accession no. AF159881).

Structure of TcPPase

The *TcPPase* ORF encodes 816 amino acids with a predicted mass of 85 kDa (Figure 1B). Although the estimated molecular mass of the protein encoded by *TcPPase* is larger than the apparent molecular mass determined by SDS/PAGE [3], the anomalous migration of hydrophobic membrane proteins on SDS gels is not unusual [18]. The sequence-analysis program PSORT identified a possible cleavable 23-amino acid N-terminal signal peptide in TcPPase. Transmembrane topology of TcPPase was predicted using TopPredII. The results of this analysis suggested the presence of 16 membrane-spanning domains (Figure 1B).

The TcPPase amino acid sequence is 53 % identical (67 % similar) to the *Arabidopsis* pyrophosphatase sequence (Figure 1B), 45 % identical (61 % similar) to the sequence of a homologous protein from *P. falciparum*, and 36 % identical (53 % similar) to the pyrophosphatase from the phototrophic bacterium, *R. rubrum* (Figure 1B). Although there are elements of similarity throughout the length of the sequence, conservation is greatest within the predicted catalytic domain, residues 298–354 of the TcPPase sequence. This domain contains the motif DX_7KXE, found in soluble and membrane-associated pyrophosphatases [19], which has been established as the metal- and substrate-binding region by high-resolution studies of soluble pyrophosphatases from both prokaryotes and eukaryotes [20]. Also present is a triglycyl sequence that occurs in all H^+-PPase family members and that may have the potential to provide an unusually high level of local conformational change [6].

A.

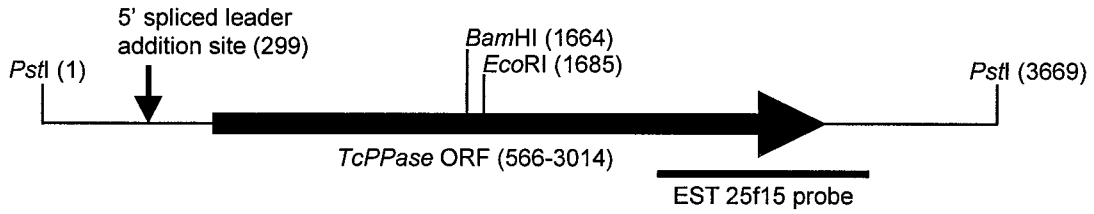

B.

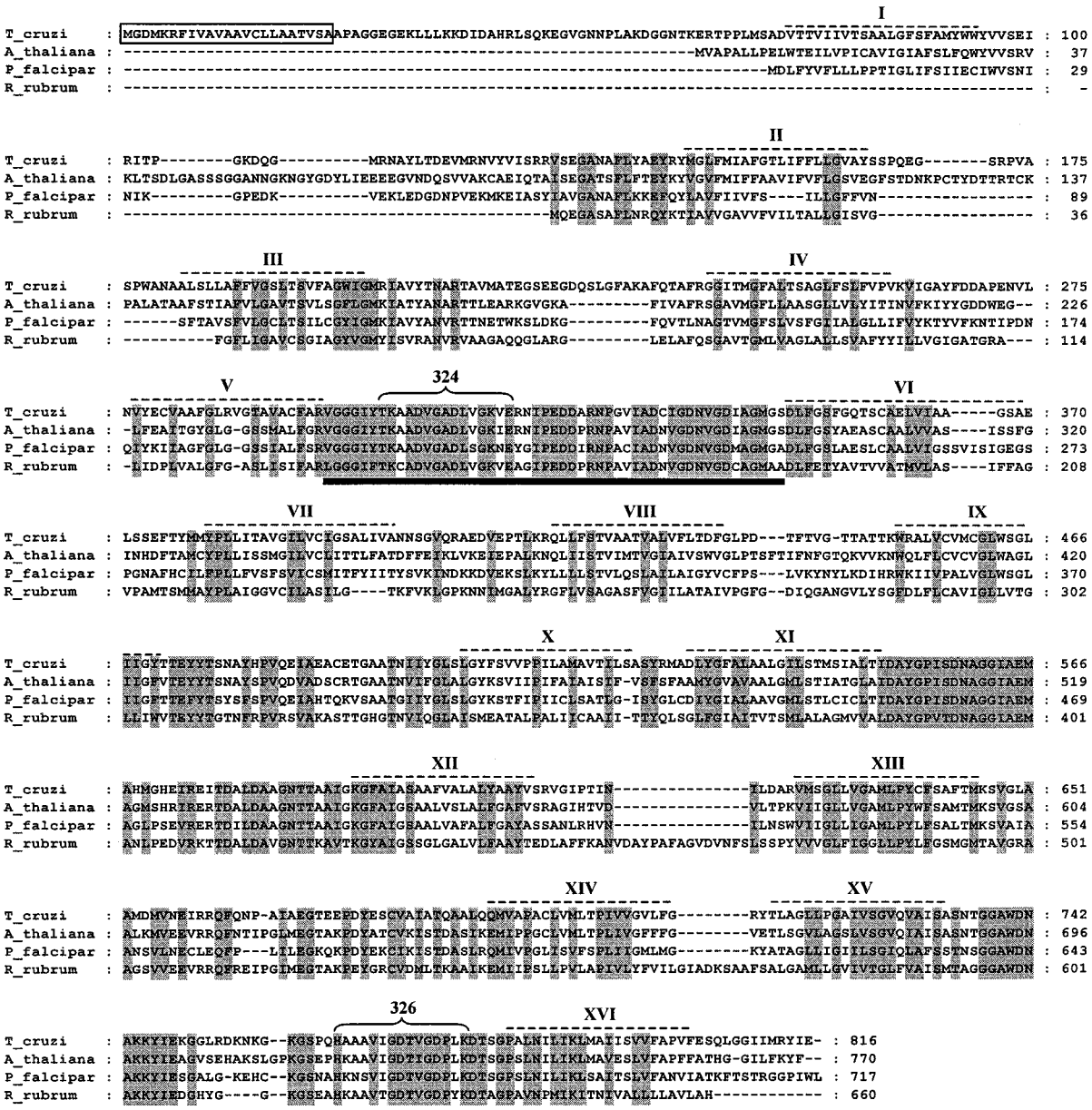

Figure 1 Scheme of the *Pst*I genomic clone and alignment of different V-H$^+$-PPases

(**A**) The 3.7-kb *Pst*I genomic subclone. The scheme shows the ORF of TcPPase (large arrow), the 5′-spliced leader-sequence-addition site and the restriction sites for *Pst*I, *Bam*HI and *Eco*RI. (**B**) CLUSTALW alignment of V-H$^+$-PPases from *T. cruzi* (GenBank accession no. AF159881), *A. thaliana* (AC005679), *P. falciparum* (AF115766) and *R. rubrum* (AAC38615). Similar residues are shaded. Amino acid residues not present within other sequences are denoted by dashes. The predicted catalytic domain is underlined, the predicted cleavable N-terminal signal sequence in the *T. cruzi* is boxed, the transmembrane domains in the *T. cruzi* sequence predicted by TopPredII (I–XVI) are indicated by dashed lines and the positions of the recognition sequences for antibodies PAB_{TK} (324) and PAB_{HK} (326) are also indicated.

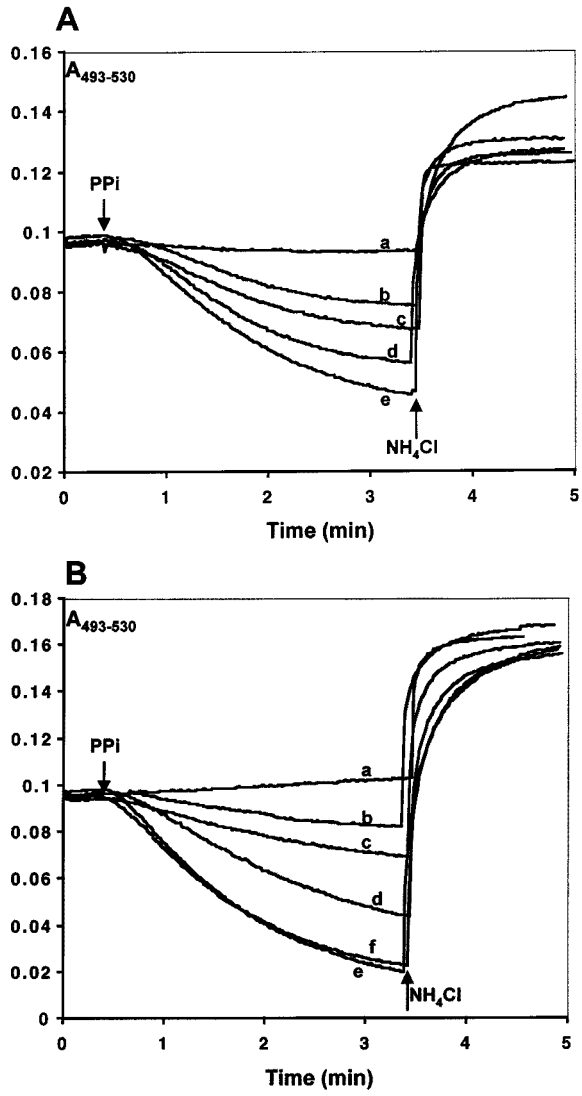

Figure 2 Inhibition of *T. cruzi* H+-PPase activity by DCCD and NEM

PP_i-driven proton pumping was assayed in permeabilized *T. cruzi* epimastigotes using Acridine Orange in a dual-wavelength spectrophotometer. Decrease in absorbance indicates increasing organelle acidity. PP_i (0.1 mM) and NH_4Cl (10 mM) were added at the points indicated. Inhibitors were added 5 min prior to PP_i. (**A**) DCCD: trace a, 1 mM; trace b, 500 μM; trace c, 200 μM; trace d, 100 μM; trace e, no inhibitor. (**B**) NEM: trace a, 40 μM; trace b, 20 μM; trace c, 15 μM; trace d, 12 μM; trace e, 5 μM; trace f, no inhibitor.

The motif TEYYTS, which is found right after transmembrane segment IX (amino acids 472–478), is also conserved in TcPPase. It has been shown that the mutation of glutamate to glutamine in this motif in the *A. thaliana* sequence uncouples H^+ transport from pyrophosphatase activity [21].

The catalytic domain includes Asp^{338}, a residue determined biochemically to be a binding site for the carbodi-imide DCCD in the *Vigna radiata* enzyme ([22], equivalent position Asp^{283}). One of the two carboxylic residues of the *A. thaliana* V-H+-PPase, Asp^{504}, determined by site-directed mutagenesis to be the site for inhibitory DCCD binding [23], is also conserved in the *T. cruzi* sequence (Asp^{551} of TcPPase). Another residue present in *A. thaliana* that is present in TcPPase is Cys^{634} of cytosolic loop VII (Cys^{680} of the TcPPase). Cys^{634} is essential for inhibition of the enzyme by maleimides but not for catalysis [21].

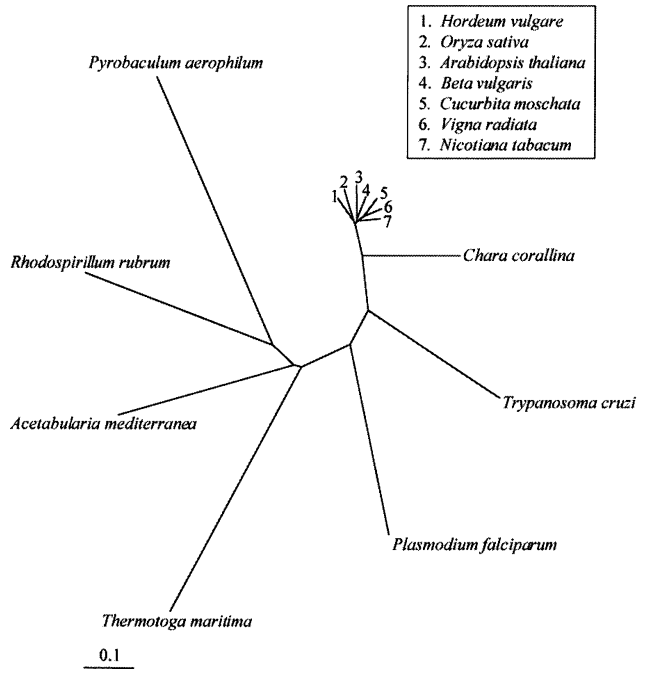

Figure 3 Unrooted distance tree based upon V-H+-PPase peptide sequences

Sequences from archaea *Pyrobaculum aerophilum* (GenBank accession no. AAF01029), thermophilic bacterium *Thermotoga maritima* (AAD35267), marine alga *Acetabularia mediterranea* (BAA83103), phototrophic bacterium *R. rubrum* (AAC38615), apicomplexan parasite *P. falciparum* (AF115766), kinetoplastid *T. cruzi* (AF159881), giant freshwater alga *Chara corallina* (AB018529) and the vascular plants *Oryza sativa* (AB012765), *Hordeum vulgare* (D13472), *Nicotiana tabacum* (X83729), *Vigna radiata* (AB009077), *Cucurbita moschata* (D86306), *A. thaliana* (AC005679) and *Beta vulgaris* (L32791). The positions of plant sequences are indicated by numbers (1–7) for clarity. The bar indicates a branch length corresponding to 0.1 substitutions per site. Distances were computed using the Dayhoff/PAM matrix within protdist and an unrooted tree was produced by neighbour joining.

Inhibition by DCCD and NEM of *T. cruzi* H+-PPase activity

Given the presence of apparent binding sites for DCCD and maleimides (NEM) in the TcPPase sequence, we wished to confirm that these compounds inhibited H+-PPase activity in *T. cruzi*. This was assayed by a dual-wavelength spectrophotometric method (Figure 2). In this assay, as organelles acidify following PP_i addition, they accumulate the weak base Acridine Orange, which dimerizes and changes its spectral properties. A decrease in absorbance at 493–530 nm indicates increasing organelle acidity. This decrease was reversed by the addition of the weak base NH_4Cl, which neutralizes the pH gradient across organelle membranes [24]. Both DCCD (Figure 2A) and NEM (Figure 2B) inhibited H+-PPase activity in a dose-responsive manner. Plots of log(percentage inhibition of initial rate of $A_{493-530}$ decrease) versus log(inhibitor concentration) using the combined data from two experiments gave I_{50} values of 200 μM (DCCD) and 13 μM (NEM).

Phylogenetic analysis of available V-H+-PPase sequences

A CLUSTALW alignment of V-H+-PPase peptide sequences from an archean, a thermophilic bacterium, a marine alga, a phototrophic bacterium, an apicomplexan, a kinetoplastid, the giant freshwater alga *Chara corallina* and several vascular plants was used as the basis for the generation of a distance tree (Figure 3). A bootstrap analysis of the consensus of 100 possible

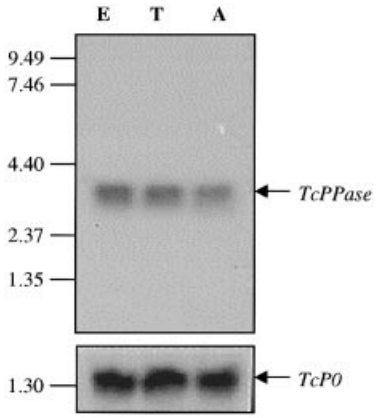

Figure 4 Expression of *TcPPase* mRNA in epimastigote (E), trypomastigote (T) and amastigote (A) forms of *T. cruzi*

(Upper panel) Poly(A)$^+$ RNA (3 μg/lane) was electrophoresed, blotted and probed at high stringency with a ^{32}P-labelled probe corresponding to the entire *TcPPase* ORF. Size markers (kb) are indicated on the left. Approximately equal amounts of RNA were observed in the three lanes under UV light. (Lower panel) The membranes were stripped and reprobed with a ^{32}P-labelled PCR fragment of the *TcP0* gene from *T. cruzi* as control. Exposure time was 48 h for the upper panel and 5 h for the lower panel.

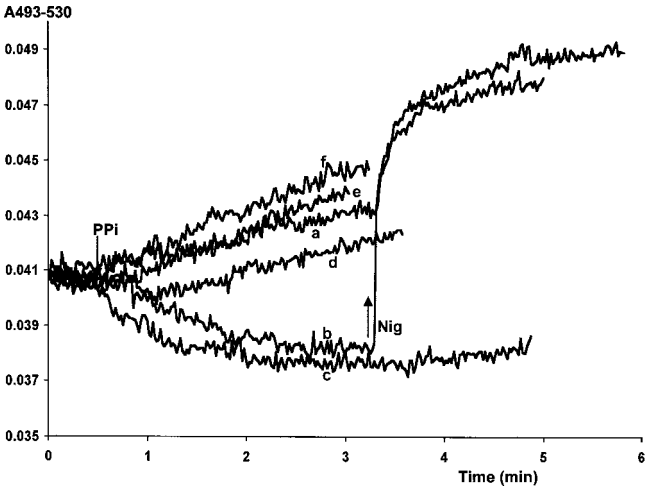

Figure 5 PP_i-driven proton transport in yeast homogenates

Membrane fractions of transformed yeast were assayed as described in Materials and Methods. Traces a–d, strain pYES2-816-H_6 (containing a construct of the complete ORF of the TcPPase with a 6 × His tag; 70 μg of protein); trace e, strain pYES2 (containing the vector alone; 220 μg of protein); trace f, strain pYES2-747-H_6 (containing a construct lacking the putative signal sequence, 270 μg of protein). Experiment in trace d additionally contained 20 μM AMDP. PP_i (0.1 mM) was added where indicated in traces b–f, and 2 μM nigericin (Nig) in traces a and b.

neighbour-joined trees indicated a high degree of internal stability for the tree (results not shown). Within the tree, the vascular plants are tightly clustered, whereas sequences from all other species (including *T. cruzi*) are much more divergent, each present on a distinct branch. The *T. cruzi* branch is closer to the vascular-plant cluster and the branch containing *Chara*, a precursor to land plants, than any of the other pyrophosphatase sequences included in the analysis.

Expression of *TcPPase*

In order to confirm the transcription of the *TcPPase* gene and determine the sequence of the 5′ end of the transcript, reverse transcriptase PCR was performed as described in the Materials and methods section. Sequence analysis of the product indicated that it was derived from the *TcPPase* gene and that the predicted initiation codon of the ORF was preceded by 268 bp of 5′-untranslated sequence. In addition, Northern-blot analysis showed the presence of a single *TcPPase* transcript of approx. 3.7 kb in each of the three life stages of *T.cruzi* (Figure 4, upper panel). Analysis of the 3.7-kb band by densitometry indicated that the *TcPPase* gene is expressed at similar levels in all stages of *T. cruzi*.

Analysis of TcPPase expressed in yeast

Membrane fractions from yeast transformed with *TcPPase* were assayed for H$^+$-PPase activity using Acridine Orange, as above. In the absence of PP_i, the absorbance drifted upwards slowly (Figure 5, trace a). When PP_i was added (Figure 5, traces b and c) the absorbance declined, indicative of organelle acidification. That this was genuine H$^+$-PPase activity was confirmed first by the reversal of the absorbance decline by the proton ionophore nigericin (Figure 5, trace b) and secondly by the inhibition of the decline by the specific H$^+$-PPase inhibitor AMDP (Figure 5, trace d). When preparations from yeast transformed with vector alone (Figure 5, trace e) or with vector with the insert for the truncated 747-amino acid-encoding *TcPPase* (Figure 5, trace f) were used, no absorbance decrease was noted upon addition of PP_i.

DISCUSSION

Our laboratory has previously reported the detection, using H$^+$-transport and PP_i-hydrolysis assays, of a V-H$^+$-PPase activity in different stages of *T. cruzi*. The V-H$^+$-PPase was localized to acidocalcisomes and the plasma membrane using subcellular fractionation and immunochemical techniques employing antibodies against the plant enzyme [3]. In this work, we have demonstrated that a gene, *TcPPase*, encoding a functional V-H$^+$-PPase, is present in the *T. cruzi* genome. This is the first report of a gene encoding a functional V-H$^+$-PPase that is not of plant, algal or bacterial origin. The sequence of a probable V-H$^+$-PPase from *P. falciparum* has been deposited in GenBank (accession no. AF115766), but no expression studies have been published. Among pyrophosphatases sequenced so far, TcPPase is the largest, with 816 amino acids. This is largely due to a longer N-terminal region compared with other pyrophosphatases (Figure 1B). The presence of a putative N-terminal leader sequence suggests that this protein is processed in the endoplasmic reticulum, and is trafficked to a location or locations within the secretory pathway. Therefore, the acidocalcisome may represent a branch of this pathway.

The *T. cruzi* V-H$^+$-PPase cross-reacted with polyclonal antibodies against keyhole-limpet haemocyanin-conjugated peptides corresponding to the catalytic domain (TKAADVGADLVG-KIE) and the C-terminal tail (HKAAVIGDTIGDPLK) of the *A. thaliana* V-H$^+$-PPase [3]. In agreement with this, sequences recognized by both antibodies PAB_{TK} (324) and PAB_{HK} (326) [25] were conserved in TcPPase, except for one conservative substitution in the first peptide motif (Ile to Val) and two substitutions in the second (Ala to Lys and Ile to Val).

The number and location of transmembrane domains predicted by TopPredII (Figure 1B) is in agreement with models predicted for V-H$^+$-PPase enzymes from *Arabidopsis* and *Pyrobaculum aerophilum* [7], except for the predicted presence of

membrane span XVI in TcPPase which would cause the short (13-residue) C-terminal tail of the protein to be on the same side of the membrane as the N-terminus. Drozdowicz et al. [7] did not include this most C-terminal transmembrane domain in their model and as a result predicted a much longer C-terminal tail on the opposite side of the vacuolar membrane from the N-terminus. Based on C-terminal aequorin fusions, it has been suggested that the C-terminal tail of the V-H^+-PPase of *Arabidopsis* is on the cytoplasmic face of the vacuolar membrane [26]. However, without confirmation of the correct (i.e. functional) insertion of the fusion protein in the vacuolar membrane it is not possible to know if the orientation of the fusion protein is the true orientation of the native V-H^+-PPase. It must be emphasized that results of analyses with programs such as TopPredII are highly speculative and while they may be useful tools for comparing sequences and making predictions about membrane topology, they cannot be relied on for a definitive answer.

We found that DCCD and NEM were effective against the *T. cruzi* H^+-PPase activity (Figure 2). This is in agreement with the presence of potential inhibitory binding sites for both DCCD (Asp^{338}, Asp^{551}) and NEM (Cys^{680}) in the TcPPase sequence. In other pyrophosphatases, DCCD binds to aspartate or glutamate residues which are involved in proton transport [23,27]; NEM binds to a cysteine residue that is not essential for activity [21] and is absent from the recently described *Pyrobaculum* sequence [7]. Compared with the results we obtained before with *Leishmania donovani* H^+-PPase, DCCD showed similar activity, whereas NEM was about 10-fold more potent [10].

The comparison of previously identified V-H^+-PPase sequences with TcPPase is described in the distance tree shown in Figure 3. Apart from the clustered vascular plant sequences, all other V-H^+-PPase sequences appear on distinct branches. This arrangement reflects the relatively high levels of sequence divergence between the non-plant species. Based on what has been determined about the location and composition of the catalytic domain of this family of enzymes, and the positions of other functionally important residues within the enzymes, it seems that the changes in sequence within these regions would be tightly constrained and under high selection pressure. However, sequences within the transmembrane domains would be less sensitive to changes in sequence, provided that the hydrophobicity and helical structure were maintained. Examination of alignments of V-H^+-PPase protein sequences, such as that shown in Figure 1B, is illustrative of this phenomenon since most of the highly variable regions of the sequence are found in the predicted transmembrane domains and in the predicted loops on the extracytosolic face of the membrane. Sequencing of ribosomal RNA [28] and proteins [29] has shown that the trypanosomatid lineage represents an ancient branch in eukaryotic evolution. It is therefore not surprising that trypanosomatids possess several plant-like enzymes. Previously described examples of this include the presence of an electron-chain alternative terminal oxidase [30], microtubule structure [31] and sterol biosynthesis [32].

Heterologous expression of the cDNA encoding the V-H^+-PPase from *T. cruzi* in the yeast *S. cerevisiae* resulted in the production of an intracellularly localized enzyme that was similar to the endogenous *T. cruzi* activity with respect to H^+ translocation and inhibition by AMDP [3]. On comparing the H^+-translocating activity of the yeast membrane fraction (Figure 5) and the *T. cruzi* permeabilized cells or isolated acidocalcisomes [3] it is evident that the activity was much lower. This may be due to low expression or instability, or perhaps not all the heterologously expressed V-H^+-PPase was transport competent. A lower coupling efficiency of V-H^+-PPase has been reported for the enzyme from *A. thaliana* expressed in *S. cerevisiae*, and this was attributed to a combination of factors such as incomplete oligomerization of the heterologously expressed enzyme and/or non-productive insertion of pump monomers into the membrane [21]. As inferred for the plant enzyme [33], the TcPPase may be active only as a dimer. Immunoblotting of extracts from yeast expressing the *T. cruzi* enzyme (results not shown) also indicated the presence of large amounts of aggregated V-H^+-PPase in the transformed yeast. This aggregation may be due to mislocalization, and is likely to result in inactive protein.

In conclusion, our results indicate that the V-H^+-PPase of *T. cruzi* is an enzyme with no counterpart in mammalian cells. Analysis of its role in parasite survival and multiplication will determine its suitability as a possible drug target.

We thank Philip A. Rea for the gift of AMDP, Lena Aslund for the 25f15 cDNA and Linda Brown for technical assistance. This work was supported by National Institutes of Health grant AI-23259 to R. D.

REFERENCES

1 World Health Organization (1997) Tropical Disease Research: progress 1995–1996, in Thirteenth Programme Report, UNDP/World Bank/World Health Organization Special Programme for Research and Training in Tropical Diseases, World Health Organization, Geneva

2 Kirchhoff, L. V. (1993) American trypanosomiasis (Chagas' disease) – a tropical disease now in the United States. New Engl. J. Med. **329**, 639–644

3 Scott, D. A., de Souza, W., Benchimol, M., Zhong, L., Lu, H.-G., Moreno, S. N. J. and Docampo, R. (1998) Presence of a plant-like proton-pumping pyrophosphatase in acidocalcisomes of *Trypanosoma cruzi*. J. Biol. Chem. **273**, 22151–22158

4 Docampo, R. and Moreno, S. N. J. (1999) Acidocalcisome: a novel Ca^{2+} storage compartment in trypanosomatids and apicomplexan parasites. Parasitol. Today **15**, 443–448

5 Rea, P. A. and Poole, R. J. (1993) Vacuolar H^+-translocating pyrophosphatase. Annu. Rev. Plant Physiol. Plant Mol. Biol. **44**, 157–180

6 Baltscheffsky, M., Schultz, A. and Baltscheffsky, H. (1999) H^+-PPases: a tightly membrane-bound family. FEBS Lett. **457**, 527–533

7 Drozdowicz, Y. M., Lu, Y.-P., Patel, V., Fitz-Gibbon, S., Miller, J. H. and Rea, P. A. (1999) A thermostable vacuolar-type membrane pyrophosphatase from the archeon *Pyrobaculum aerophilum*: implications for the origins of pyrophosphate-energized pumps. FEBS Lett. **460**, 505–512

8 Brightman, A. O., Navas, P., Minnifield, N. N. and Morré, D. J. (1992) Pyrophosphate-induced acidification of *trans* cisternal elements of rat liver Golgi apparatus. Biochim. Biophys. Acta **1104**, 188–194

9 Rodrigues, C. O., Scott, D. A. and Docampo, R. (1999) Characterization of a vacuolar pyrophosphatase in *Trypanosoma brucei* and its localization to acidocalcisomes. Mol. Cell. Biol. **19**, 7712–7723

10 Rodrigues, C. O., Scott, D. A. and Docampo, R. (1999) Presence of a vacuolar H^+-pyrophosphatase in promastigotes of *Leishmania donovani* and its localization to a different compartment from the vacuolar H^+-ATPase. Biochem. J. **340**, 759–766

11 Luo, S., Marchesini, N. and Docampo, R. (1999) A plant-like vacuolar H^+-pyrophosphatase in *Plasmodium falciparum*. FEBS Lett. **460**, 217–220

12 Rodrigues, C. O., Scott, D. A., Bailey, B. N., de Souza, W., Benchimol, M., Moreno, B., Urbina, J. A., Oldfield, E. and Moreno, S. N. J. (2000) Vacuolar proton pyrophosphatase activity and pyrophosphate in *Toxoplasma gondii* as possible chemotherapeutic targets. Biochem. J. **349**, 737–745

13 Bone, G. J. and Steinert, M. (1956) Isotopes incorporated in the nucleic acids of *Trypanosoma mega*. Nature (London) **178**, 308–309

14 Zhen, R. G., Baykov, A. A., Bakuleva, N. P. and Rea, P. A. (1994) Aminomethylenediphosphonate: a potent type-specific inhibitor of both plant and phototrophic bacterial H^+-pyrophosphatases. Plant Physiol. **104**, 153–159

15 Sambrook, J., Fritsch, E. F. and Maniatis, T. (1989) Molecular Cloning: a Laboratory Manual, 2nd edn, Cold Spring Harbor Press, Cold Spring Harbor

16 Skeiky, Y. A. W., Benson, D. R., Parsons, M., Elkon, K. B. and Reed, S. G. (1992) Cloning and expression of *Trypanosoma cruzi* ribosomal protein P0 and epitope analysis of anti-P0 autoantibodies in Chagas' disease patients. J. Exp. Med. **176**, 201–211

17 Gietz, D., St. Jean, A., Woods, R. A. and Schiestl, R. H. (1992) Improved method for high efficiency transformation of intact yeast cells. Nucleic Acids Res. **20**, 1425

18 Sarafian, V., Kim, Y., Poole, R. J. and Rea, P. A. (1992) Molecular cloning and sequence of cDNA encoding the pyrophosphate-energized vacuolar membrane proton pump of *Arabidopsis thaliana*. Proc. Natl. Acad. Sci. U.S.A. **89**, 1775–1779

19 Rea, P. A., Kim, Y., Sarafian, V., Poole, R. J., Davies, J. M. and Sanders, D. (1992) Vacuolar H^+-translocating pyrophosphatase: a new category of ion translocase. Trends Biochem. Sci. **17**, 348–353
20 Heikinheimo, P., Pohjanjoki, R., Helmimen, A., Tasanen, M., Coperman, B. S., Goldman, A., Baykov, A. and Lahti, R. (1996) A site-directed mutagenesis study of *Saccharomyces cerevisiae* pyrophosphatase. Functional conservation of the active site of soluble inorganic pyrophosphatases. Eur. J. Biochem. **239**, 138–143
21 Kim, E. J., Zhen, R.-G. and Rea, P. A. (1995) Site-directed mutagenesis of vacuolar H^+-pyrophosphatase. Necessity of Cys634 for inhibition by maleimides but not catalysis. J. Biol. Chem. **270**, 2630–2635
22 Yang, S. J., Jiang, S. S., Kuo, S. Y., Hung, S. H., Tam, H. H. and Pan, R. L. (1999) Localization of a carboxylic residue possibly involved in the inhibition of vacuolar H^+-pyrophosphatase by *N,N′*-dicyclohexylcarbodi-imide. Biochem. J. **342**, 641–646
23 Zhen, R.-G., Kim, E. J. and Rea, P. A. (1997) Acidic residues necessary for pyrophosphate-energized pumping and inhibition of the vacuolar H^+-pyrophosphatase by *N,N′*-dicyclohexylcarbodiimide. J. Biol. Chem. **272**, 22340–22348
24 Scott, D. A., Moreno, S. N. J. and Docampo, R. (1995) Ca^{2+} storage in *Trypanosoma brucei*: the influence of cytoplasmic pH and importance of vacuolar acidity. Biochem. J. **310**, 789–794
25 Kim, E. J., Zhen, R.-G. and Rea, P. A. (1994) Heterologous expression of plant vacuolar pyrophosphatase in yeast demonstrates sufficiency of the substrate-binding subunit for proton transport. Proc. Natl. Acad. Sci. U.S.A. **91**, 6128–6132
26 Knight, H., Trewavas, A. J. and Knight, M. R. (1996) Cold calcium signaling in *Arabidopsis* involves two cellular pools and a change in calcium signature after acclimation. Plant Cell **8**, 489–503
27 Solioz, M. (1984) Dicyclohexylcarbodiimide as a probe for proton translocating enzymes. Trends Biochem. Sci. **9**, 309–312
28 Cavalier-Smith, T. (1993) Kingdom protozoa and its 18 phyla. Microbiol. Rev. **57**, 953–994
29 Doolittle, R. F., Feng, D.-F., Tsang, S., Cho, G. and Little, E. (1996) Determining divergence times of the major kingdoms of living organisms with a protein clock. Science **271**, 470–477
30 Chaudhuri, M. and Hill, G. C. (1996) Cloning, sequencing, and functional activity of the *Trypanosoma brucei brucei* alternative oxidase. Mol. Biochem. Parasitol. **83**, 125–129
31 Chan, M. M.-Y., Grogl, M., Chen, C. C., Bienen, E. J. and Fong, D. (1993) Herbicides to curb human parasitic infections: in vitro and in vivo effects of trifluralin on the trypanosomatid protozoans. Proc. Natl Acad. Sci. U.S.A. **90**, 5657–5661
32 Docampo, R. and Schmuñis, G. A. (1997) Sterol biosynthesis inhibitors as potential chemotherapeutic agents against Chagas' disease. Parasitol. Today **13**, 129–130
33 Zhen, R.-G., Kim, E. J. and Rea, P. A. (1997) The molecular and biochemical basis of pyrophosphate-energized proton translocation at the vacuolar membrane. Adv. Bot. Res. **25**, 297–337

Received 11 May 2000/3 July 2000; accepted 25 July 2000